https://doi.org/10.5194/egusphere-2025-285
Preprint. Discussion started: 18 March 2025

Nonlinear effects of the stratospheric Quasi-Biennial Oscillation on ENSO modulating $PM_{2.5}$ over the North China Plain in early winter

Xiadong An[1,2,3], Wen Chen[1,2], Tianjiao Ma[1,2*], Lifang Sheng[3*]

[1]Yunnan International Joint Laboratory of Monsoon and Extreme Climate Disasters, Yunnan University, Kunming, 650500, China
[2]Yunnan Key Laboratory of Meteorological Disasters and Climate Resources in the Greater Mekong Subregion, Yunnan University, Kunming, 650091, China
[3]Department of Marine Meteorology, College of Oceanic and Atmospheric Sciences, Ocean University of China, Qingdao, 266100, China

Correspondence to: Tianjiao Ma (matianjiao@ynu.edu.cn), Lifang Sheng (shenglf@ouc.edu.cn)

Abstract. The North China Plain (NCP) experiences severe air pollution, with $PM_{2.5}$ (fine particulate matter with an aerodynamic diameter ≤ 2.5 μm) as the primary pollutant, especially in early winter (November to December). The $PM_{2.5}$ concentrations in this period is significantly modulated by the El Niño-Southern Oscillation (ENSO). In this study, we have found that the stratospheric Quasi-Biennial Oscillation (QBO) exerts a nonlinear impact on the relationship between ENSO and $PM_{2.5}$ concentrations over the NCP in early winter. During the easterly QBO (EQBO) phase, ENSO's influence on $PM_{2.5}$ concentration is stronger compared to the westerly QBO (WQBO) phase. In El Niño and EQBO years, $PM_{2.5}$ concentrations rise due to meteorological factors like a shallower boundary layer, higher relative humidity, and intensified southerly wind anomalies. Conversely, during La Niña and EQBO years, $PM_{2.5}$ levels decrease due to opposite meteorological conditions. The study attributes these changes to planetary wave dynamics. During El Niño and EQBO years, upward-propagating planetary waves in mid-latitudes enhance upper-level divergence over Eurasia, strengthening westerlies. These westerlies guide Rossby wave trains into Northeast Asia, forming a strong anomalous anticyclone that worsens air pollution over the NCP. In La Niña and EQBO years, downward-propagating planetary waves induce divergence in sub-polar regions, strengthening westerlies that facilitate La Niña-related wave trains. These wave trains trigger cyclonic circulation over Northeast Asia, improving air quality in the NCP. These findings underscore the complex interplay between ENSO, QBO, and atmospheric dynamics in shaping regional air pollution.

1 Introduction

Air pollution dominated by $PM_{2.5}$ (fine particulate matter with an aerodynamic diameter ≤ 2.5 μm) poses enormous risks to human health and socioeconomic development (e.g., Shi et al., 2021; Geng et al., 2021). The North China Plain (NCP), one of the most densely populated regions in China, has been severely troubled by $PM_{2.5}$ pollution, particularly in winter months. This has persisted despite the Chinese government's comprehensive emission control measures implemented since 2013

https://doi.org/10.5194/egusphere-2025-285
Preprint. Discussion started: 18 March 2025

(*Nature Geoscience*, 2019). Previous studies have highlighted that wintertime $PM_{2.5}$ pollution in eastern China is primarily driven by both emissions and meteorological conditions (Dang and Liao, 2019; Wu et al., 2022; Jing et al., 2023; Dai et al., 2023). Notably, the interannual variability of $PM_{2.5}$ concentrations over the NCP is largely influenced by meteorological conditions (Dang and Liao, 2019), particularly large-scale atmospheric circulation patterns and associated climate factors (An et al., 2020, 2022a, 2022b, 2023a; Wang et al., 2020; Yin et al., 2021).

The El Niño-Southern Oscillation (ENSO), the most prominent interannual variability in the atmosphere-ocean interactions globally (Bjerknes, 1969; Rasmusson and Carpenter, 1982; Philander et al., 1984), has a profound impact on global weather and climate (Alexander, 1992; Zhang et al., 1996; Wang et al., 2000; Zhang and Akimasa, 2002; Yuan, 2004; Zhou et al., 2014). Given its the crucial in shaping global weather and climate, extensive research has been conducted to explore whether ENSO influences air pollution in the NCP. For example, some studies suggested a significant relationship between ENSO and air pollution over the NCP (e.g., Chang et al., 2016; Jeong et al., 2018; Zhang et al., 2019; Xie et al., 2021; Zeng et al., 2021), while others argued there is little to no correlation (e.g., Li et al., 2017; Zhao et al., 2018; Cheng et al., 2019; He et al., 2019). Recently, building on a review of these conflicting findings, research has increasingly suggested that ENSO does indeed affect air pollution over the NCP, particularly during the November to January period (Zhao et al., 2022; An et al., 2022a, 2022b, 2023a). The physical mechanisms behind this influence are now better understood. One explanation is that ENSO impacts air pollution in the Beijing–Tianjin–Hebei region by modulating the Hadley circulation during November–December (Zhao et al., 2022). Another mechanism involves ENSO-induced wave trains along the mid- and high-latitudes pathways in the Northern Hemisphere, as well as the Indo–Pacific great circle route, which trigger a Northeast Asian anomalous anticyclone, thereby influencing air pollution over the NCP from November to January (An et al., 2022a, 2022b, 2023a). This new body of evidence helps the debate regarding the role of ENSO in air pollution over the NCP.

In addition to ENSO, the stratospheric Quasi-Biennial Oscillation (QBO) is another crucial climatic factor influencing global atmospheric circulation (Holton and Tan, 1980; Chen and Li, 2007; Wei et al., 2007; Rao et al., 2020; Cai et al., 2022; Ern et al., 2023; Kang et al., 2023; Zhang and Zhou, 2023). Both the QBO and ENSO originate in the tropics, with the former being a stratospheric phenomenon and the latter a tropospheric one. Notably, the QBO and ENSO may interact with each other in a linear manner (Wang et al., 2023), and together, they influence atmospheric circulations over the North Atlantic in winter (Ma et al., 2023) and winter climate over Eurasia (Chen et al., 2005, 2007; Ma et al., 2021; Zhang et al., 2023). For example, Ma et al. (2021) reported that the easterly QBO (EQBO) weakens East Asian winter monsoon during November–December. The weakening of the monsoon tends to deteriorate air quality in the NCP (An et al., 2020; Zhao et al., 2021). This raises the question of whether the QBO modulates the relationship between ENSO and air pollution over the NCP during early winter.

In this study, we examine the evidence that the QBO nonlinearly modulates the relationship between ENSO and $PM_{2.5}$ concentrations over the NCP during early winter (November–December, hereafter referred as ND). We analyse the characteristics of $PM_{2.5}$ concentrations and the associated meteorological conditions during different ENSO and QBO composites and explore the underling physical mechanisms. The remainder of this paper is organized as follows: Section 2 describes the datasets and methods; Section 3 discusses nonlinear effects of the QBO on the connection between ENSO and

https://doi.org/10.5194/egusphere-2025-285
Preprint. Discussion started: 18 March 2025

$PM_{2.5}$ concentration; The underlying physical mechanisms are explored in section 4; Finally, a brief summary and discussion of the results are provided in section 5.

2 Data and methods

2.1 Data

Monthly $PM_{2.5}$ data, provided by Yang (2020), has a horizontal resolution of 1°×1° and covers the period from 1980 to 2019. It can be accessed at https://zenodo.org/records/4293239 (last access: 9 April 2021). This dataset has been widely used in studies of air pollution in China (e.g., An et al., 2022b, 2022c; Zhang et al., 2023, 2024). According to Li et al. (2021), the monthly $PM_{2.5}$ concentrations show excellent agreement with ground-based measurements, with a coefficient of determination of 0.95 and a mean relative error of 12%. To further validate the results based on $PM_{2.5}$ data provided by Yang (2020), we also used monthly $PM_{2.5}$ data provided by Zhong et al. (2022a, 2022b).

The monthly atmospheric reanalysis products, including geopotential height, zonal and meridional winds, and relative humidity, were obtained from the NCEP–DOE AMIP-II reanalysis (Kanamitsu et al., 2002), provided by the National Centers for Environmental Prediction (NCEP)/National Center for Atmospheric Research (NCAR). These reanalysis products have a horizontal resolution of 2.5°×2.5° and a vertical resolution of 17 levels from 1000 hPa to 10 hPa, starting from 1979. Monthly boundary layer height data were downloaded from the Fifth major global reanalysis (ERA5), produced by the European Centre for Medium-Range Weather Forecasts (ECMWF), with a horizontal resolution of 1.0°×1.0° at a single pressure since 1959 (Hersbach et al., 2018). The ENSO index was obtained from Climate Prediction Center (CPC) of the National Weather Service (NWS) in the United States and the QBO index was provided by Freie Universität Berlin (FUB).

2.2 Methods

To capture the characteristics of the QBO, this study defines the 10-hPa zonal wind speed as the QBO index. Wind speeds greater than 2 m s^{-1} and less than −2 m s^{-1} are categorized as the westerly QBO phase (WQBO) and EQBO, respectively. The classification of cold and warm phases of ENSO events is based on the National Climate Centre of China website (http://cmdp.ncc-cma.net/cn/index.htm) and the website provided by Jan Null (https://ggweather.com/enso/oni.htm). When selecting ENSO events, the focus is on whether the periods from October to December and November to January correspond to El Niño or La Niña. This study particularly emphasizes the season of November and December (ND), as highlighted in previous studies (Ma et al., 2021; An et al., 2023a). Figure 1 illustrates the spatial and temporal evolution of the QBO and ENSO during the research period of this paper. The different combinations of ENSO and the QBO are summarized in Table 1.

https://doi.org/10.5194/egusphere-2025-285
Preprint. Discussion started: 18 March 2025

In this study, we apply the bootstrap method (Austin and Tu, 2004) to obtain more samples. Specifically, we randomly resample from the selected data, allowing repeated selection of any sample. This process is repeated 1,000 times to compute the mean of the resampled samples.

To examine the propagation of tropospheric Rossby wave trains responsible for air pollution over the NCP, the horizontal wave activity flux is calculated following the method outlined by Takaya and Nakamura (2001):

$$\boldsymbol{W} = \frac{pcos\varphi}{2|\boldsymbol{U}|}\cdot\begin{pmatrix} \frac{U}{a^2cos^2\varphi}\left[\left(\frac{\partial\psi'}{\partial\lambda}\right)^2 - \psi'\frac{\partial^2\psi'}{\partial\lambda^2}\right] + \frac{V}{a^2cos\varphi}\left[\frac{\partial\psi'}{\partial\lambda}\frac{\partial\psi'}{\partial\varphi} - \psi'\frac{\partial^2\psi'}{\partial\lambda\partial\varphi}\right] \\ \frac{U}{a^2cos\varphi}\left[\frac{\partial\psi'}{\partial\lambda}\frac{\partial\psi'}{\partial\varphi} - \psi'\frac{\partial^2\psi'}{\partial\lambda\partial\varphi}\right] + \frac{V}{a^2}\left[\left(\frac{\partial\psi'}{\partial\varphi}\right)^2 - \psi'\frac{\partial^2\psi'}{\partial\varphi^2}\right] \end{pmatrix}, \quad (1)$$

where $\boldsymbol{W}$ is the wave activity flux with unit of $m^2\ s^{-2}$; ψ (= Φ/f) is the geostrophic stream function, in which Φ (m) is geopotential height, f (= $2\Omega\sin\phi$) is the Coriolis parameter; λ is the longitude; φ is the latitude; a is the radius of the earth; p is the normalized pressure (pressure per 1000 hPa); $\boldsymbol{U}$ (= (U, V); m s^{-1}) is the basic flow. The primes denote anomalies after the removal of the climatological mean.

To diagnose the interaction between the troposphere and stratosphere, we computed the Eliassen-Palmer (EP) flux (Edmon et al., 1980; Andrews et al., 1987). The quasi-geostrophic EP flux in spherical geometry was calculated following the method outlined by Chen et al. (2013):

$$F_y = -\rho acos\varphi\overline{u'v'}, \quad (2)$$

$$F_z = \rho acos\varphi\frac{Rf}{HN^2}\overline{v'T'}, \quad (3)$$

$$D_F = \frac{\nabla\cdot\vec{F}}{\rho acos\varphi}, \quad (4)$$

where $\vec{F}(F_y, F_z)$ is the components of the EP flux; D_F is the EP flux divergence; ρ is the air density; a is the earth's radius; φ is the latitude; R is the gas constant; f is the Coriolis parameter; H is a constant-scale height (7 km); N is the buoyancy frequency; u and v are the zonal and meridional wind; T is the air temperature; the primes and overbars denote zonal deviations and means. The EP flux is scaled according to Edmon et al. (1980) for pressure coordinates.

3 Nonlinear effects of the QBO on the relationship between ENSO and $PM_{2.5}$ concentrations

Figure 2 shows the distributions of $PM_{2.5}$ concentration anomalies in eastern China during different combinations of ENSO and QBO events. It is clearly that during La Niña and the EQBO phase, there is a significant reduction in $PM_{2.5}$ concentration over the NCP, while during El Niño and EQBO composites, $PM_{2.5}$ concentrations increase substantially (Figs. 2a, 2c and 3). However, regardless of whether is La Niña or El Niño, these is no significant change in $PM_{2.5}$ concentrations over the NCP during the WQBO phase (Fig. 2b and 2d). This suggests a potential relationship between the EQBO and $PM_{2.5}$ concentrations over the NCP in early winter during ENSO events. Previous studies have indicated that ENSO events significantly modulate early-winter air pollution (i.e., higher $PM_{2.5}$ concentration) over the NCP (Chang et al., 2016; Zhao et

https://doi.org/10.5194/egusphere-2025-285
Preprint. Discussion started: 18 March 2025

al., 2022; An et al., 2022a, 2022b, 2023a). It is noteworthy that in non-ENSO years, regardless of whether the QBO is in easterly or westerly phase, no significant change in $PM_{2.5}$ concentration is observed (Fig. 2e and f), indicating that ENSO events are the key factor driving changes in $PM_{2.5}$ concentrations over the NCP. As shown in Fig. 2h, the ENSO index exhibits a significant positive correlation with $PM_{2.5}$ concentrations over the NCP. Interestingly, when the linear relationship between the QBO and $PM_{2.5}$ concentrations is removed, the relationship between ENSO and $PM_{2.5}$ remains almost identical (Fig. 2g and 2f), suggesting that while the QBO does not directly influence $PM_{2.5}$ concentrations, it significantly nonlinearly modulates the relationship between ENSO and $PM_{2.5}$ concentrations over the NCP in early winter. The results based on $PM_{2.5}$ data provided by Zhong et al. (2022) also support these findings (Fig. S1). The now question is whether the observed changes in $PM_{2.5}$ concentrations during different combinations of ENSO and EQBO phases can be attributed to concurrent changes in meteorological conditions associated with both ENSO and EQBO during the same period.

To investigate the mechanisms through which meteorological conditions related to ENSO and the EQBO modulate $PM_{2.5}$ concentrations over the NCP in early winter, we examine the distributions of 850-hPa wind fields, 925-hPa relative humidity, and atmospheric boundary layer height during ENSO and EQBO composites. The results clearly show that during La Niña and EQBO composites (and similarly, El Niño and EQBO composites), the lower-level anomalous wind fields over the NCP shift distinctly towards northerly (southerly) winds, which correspond to an intensification (weakening) of the East Asian winter monsoon (Fig. 3). This shift in winds enhances (diminishes) atmospheric dispersion conditions for air pollutants, leading to decrease (increase) in $PM_{2.5}$ concentrations, as observed over the NCP during early winter in La Niña and EQBO composites (El Niño and EQBO composites). Additionally, an analysis of atmospheric boundary layer height anomalies reveals that during La Niña and EQBO composites (El Niño and EQBO composites), the northern part of the NCP experiences higher (lower) boundary layer heights (Fig. 4a and 4c), which favors (hinders) the vertical dispersion conditions of air pollutants in the region, ultimately promoting the accumulation of $PM_{2.5}$. In contrast, during La Niña and WQBO composites (El Niño and WQBO composites), no significant change in atmospheric boundary layer height is observed over the NCP, resulting in little to no change in $PM_{2.5}$ concentrations.

In addition to dynamic factors, atmospheric thermal conditions (i.e., humidity) also contribute to the variation in $PM_{2.5}$ concentrations over the NCP during early winter, particularly in La Niña (El Niño) and EQBO composites. As shown in Figs. 4e and 4g, relative humidity over the NCP is lower (higher) during La Niña (El Niño) and EQBO composites compared to La Niña (El Niño) and WQBO composites. Previous studies have shown that higher relative humidity favors the hygroscopic growth of particulate matters (Zhou et al., 2011). An at al. (2020) reported that during episodes of severe air pollution (i.e., higher $PM_{2.5}$ concentration) in the NCP, relative humidity in the region is indeed higher. These findings suggest that lower (higher) relative humidity during La Niña (El Niño) and EQBO composites contributes to the occurrence of lower (higher) $PM_{2.5}$ concentrations over the NCP in early winter.

In summary, both atmospheric dynamic dispersion and thermal conditions during La Niña (El Niño) and EQBO composites favor lower (higher) $PM_{2.5}$ concentrations over the NCP. The remining questions are which large-scale circulation patterns modulate these meteorological conditions, and how do these relate to ENSO and the QBO.

https://doi.org/10.5194/egusphere-2025-285
Preprint. Discussion started: 18 March 2025

4 Physical mechanisms

To elucidate the physical mechanisms underlying the nonlinear modulation of the relationship between early-winter $PM_{2.5}$ concentration over the NCP and ENSO by the EQBO, we diagnosed the propagation characteristics and causes of the associated large-scale Rossby wave trains. As depicted in Fig. 6a, during La Niña and EQBO composites, northeast Asia exhibits a significant negative geopotential height anomaly at 500 hPa, corresponding to a stronger cyclonic circulation anomaly. Conversely, during El Niño and EQBO composites, northeast Asia displays a notable positive geopotential height anomaly, indicative of a strong anticyclonic circulation anomaly (Fig. 6c). An et al. (2023b) identified the cyclonic circulation anomaly in northeast Asia as a key factor leading to a decrease in $PM_{2.5}$ concentrations over the NCP during early winter. Conversely, the anticyclonic circulation anomaly in northeast Asia (referred to as the northeast Asian anticyclonic anomaly (NAAA)) is a crucial system responsible for the increase in early-winter $PM_{2.5}$ concentration over the NCP (Zhong et al., 2019; An et al., 2020, 2022a, 2022b, 2022c, 2023a). These circulation systems primarily influence $PM_{2.5}$ concentrations over the NCP by modulating lower-level wind fields, near-surface relative humidity, and boundary layer height. In contrast, during La Niña and WQBO composites (El Niño and WQBO composites), the intensity of the cyclonic circulation anomaly (anticyclonic circulation anomaly) in northeast Asia is weaker, and its position is shifted eastward. These changes are unfavourable for inducing changes in meteorological conditions that affect $PM_{2.5}$ concentrations in the NCP.

Delving deeper, we find that during La Niña and EQBO composites, the northeast Asian cyclonic anomaly is driven by a Rossby wave train originating from northeast Pacific and traversing the Eurasian sub-polar region (Fig. 6a). Similarly, the NAAA during El Niño and EQBO composites results from a Rossby wave train passing through the mid- and lower-latitudes of the Eurasian continent, also originating from northeast Pacific (Fig. 6c). Previous studies have indicated that ENSO events can trigger wave trains similar to those illustrated in Figs. 6a and 6c (Yu and Sun, 2020; An et al., 2022a, 2023a). Notably, the position of the Rossby wave train in La Niña and EQBO composites is more northerly compared to during El Niño and EQBO composites, which may be linked the positioning of the waveguides that channel the energy of these wave trains (Hoskins and Ambrizzi, 1993). As a contrast, during La Niña and WQBO composites (El Niño and WQBO composites), the signals associated with ENSO struggle to reach the northeast Asia region, resulting in weaker and more eastward-shifted circulation anomalies (Figs. 6b and 6d). The distribution of wave activity flux and the anomalous streamfunction further corroborate these results (Fig. 7). Specifically, during La Niña and EQBO composites (El Niño and EQBO composites), ENSO-related signals are more likely to propagate into the northeast Asia region, inducing significant circulation anomalies in the region (Figs. 6 and 7), which in turn affect $PM_{2.5}$ concentration anomalies over the NCP by modulating local meteorological conditions (Figs. 2–5).

The strong zonal wind acts as a waveguide for the propagation of Rossby wave trains (Hoskins and Ambrizzi, 1993). To further understand why the Rossby waves associated with ENSO can propagate into northeast Asia during ENSO and EQBO composites, we examine the zonal wind distribution in the upper troposphere. As shown in Fig. 8, compared to La Niña and

https://doi.org/10.5194/egusphere-2025-285
Preprint. Discussion started: 18 March 2025

WQBO composites, there is a significant positive zonal wind anomaly at 250 hPa over the high latitudes of the North Atlantic and the Eurasian continent (purple box in Fig. 8a) in La Niña and EQBO composites, corresponding to an acceleration of westerlies in the subpolar region. This is conducive to the downward dispersion of Rossby wave energy in that region. Similarly, compared to La Niña and WQBO composites, El Niño and EQBO composites show a notable positive zonal wind anomaly in the mid- (purple box on the top in Fig. 8c) and lower- latitudes (purple box on the below in Fig. 8c) of the Eurasian continent, indicating a strengthening of westerlies in these regions, which supports the downstream propagation of Rossby waves. Examining the vertical profile of zonal winds in the Northern Hemisphere (Fig. 9a–d) and over the Eurasian continent (Fig. 9e–h) during different ENSO and QBO composites reveals that the anomalous zonal winds extend across the mid- and upper- levels of the troposphere and lower stratosphere in ENSO and EQBO composites (Figs. 9a, 9c 9e and 9g), implying a potential connection between the troposphere and stratosphere via troposphere-stratosphere interactions. It is worth noting that the focal point of this study, the QBO, represents a classic climatic factor in the stratosphere. The QBO can modulate the propagation of planetary waves between the troposphere and stratosphere (Ma et al., 2021; Koval et al., 2022).

Given that a close connection between the OBO and extratropical circulations (Holton and Tan, 1980; Kinnersley, 1999; Kinnersley and Tung, 1999; Chen et al., 2007), the propagation of planetary waves, as revealed by the EP flux, indicates that in La Niña and EQBO composites, there is a noticeable anomalous propagation of planetary waves in the high latitudes of the Northern Hemisphere, leading to divergence in the upper levels of the troposphere and thus enhancing zonal westerly winds in that region (Figs. 8a, 9e and 10a). During El Niño and EQBO composites, there is anomalous upward propagation of planetary waves in the high latitudes of the Northern Hemisphere, with components in the equatorial region diverging in the mid-latitudes, resulting in a positive zonal wind anomaly (Figs. 8c, 9g and 10c). These accelerated westerly winds facilitate the propagation of Rossby wave energy, enabling the wave trains associated with ENSO to reach northeast Asia and ultimately induce anomalous circulations in that region. These anomalous circulations, by modulating local meteorological elements, lead to changes in $PM_{2.5}$ concentrations over the NCP.

5 Discussions and conclusions

This study, based on $PM_{2.5}$ data constructed by machine learning and reanalysis datasets, employs composite analysis methods to investigate the physical mechanisms underlying the modulation role of the relationship between ENSO and $PM_{2.5}$ concentrations in early winter over the NCP by the QBO. The results show that the QBO nonlinearly modulates the ENSO-$PM_{2.5}$ connection. Specifically, during the EQBO phase, the influence of ENSO on $PM_{2.5}$ concentrations over the NCP is more pronounced compared to the WQBO phase. For example, during El Niño and EQBO composites, there is a noticeable increase in early-winter $PM_{2.5}$ concentrations over the NCP relative to climatology, while during La Niña and EQBO composites, a decrease is observed. These changes in $PM_{2.5}$ concentrations do not occur in ENSO and WQBO composites. Further results show that these changes in $PM_{2.5}$ concentrations are driven by meteorological conditions associated with

https://doi.org/10.5194/egusphere-2025-285
Preprint. Discussion started: 18 March 2025

ENSO and EQBO, including a shallower boundary layer, higher relative humidity, and stronger southerly wind anomalies during El Niño and EQBO composites (opposite conditions occur during La Niña and EQBO composites).

Through the diagnosis of Rossby waves and planetary waves based on wave activity flux and EP flux, it is found that during El Niño and EQBO years, upward-propagating planetary waves in the mid-latitudes of the Northern Hemisphere induce upper-level divergence over the Eurasia hinterland, favouring the strengthening of westerlies. Serving as a waveguide, these westerlies facilitate the propagation of El Niño-related Rossby wave trains into northeast Asia, leading to a strong northeast Asian anomalous anticyclone in the region. This anticyclonic anomaly elevates $PM_{2.5}$ concentrations over the NCP by changing the aforementioned meteorological conditions. Conversely, during La Niña and EQBO years, downward-propagating planetary waves induce mid- and upper-level divergence in the sub-polar regions of the Northern Hemisphere, enhancing westerlies in that area. Acting as a waveguide, these westerlies support propagation of La Niña-related wave trains into northeast Asia, triggering cyclonic circulation within the region. This cyclonic circulation leads to a decrease in $PM_{2.5}$ concentrations over the NCP by altering meteorological conditions mentioned as previously described. In contrast, WQBO does not support the propagation of the aforementioned planetary waves, and thus does not provide convenience for the propagation of ENSO-related Rossby waves in the troposphere. Consequently, there are no significant atmospheric circulation anomalies in Northeast Asia, and that the variation in $PM_{2.5}$ concentrations over the NCP is less pronounced.

Most notably, An et al. (2023a) found that El Niño and Arctic sea-ice increases have a synergistic effect on the Northeast Asian anomalous anticyclone, which in turn contributes to $PM_{2.5}$ pollution in early winter over the NCP. They developed a simple linear model that can skilfully predict the Northeast Asian anomalous anticyclone up to one month in advance. However, when considering the QBO, the newly developed prediction model exhibits enhanced performance (Fig. S2). For instance, the correlation coefficient between the new linear model and the raw index is 0.64 (significant at 0.05 level with an effective degree of freedom of 14), surpassing the 0.61 correlation coefficient (significant at 0.05 level with an effective degree of freedom of 14) obtained when the QBO is not considered. This further emphasizes the important role of the QBO in influencing the key atmospheric circulation systems responsible for variations of $PM_{2.5}$ concentrations over the NCP.

In addition, An et al. (2020, 2022a, 2022b, 2022c) pointed out that when the NCP experiences air pollution, southern China tends to suffer from heavy rainfall, resulting in the phenomenon of “Southern Rainfall-Northern Haze” in eastern China. This southern rainfall is conducive to air pollution over the NCP by triggering an anomalous anticyclone and promoting convective feedback. Interestingly, during El Niño and EQBO composites (La Niña and EQBO composites), rainfall indeed occurs in southern China (Fig. S3). This suggests that the QBO also nonlinearly modulates the connection between ENSO and the “Southern Rainfall-Northern Haze” phenomenon in eastern China.

It is important to note that while this study highlights the nonlinear role of the QBO in modulating the connection between ENSO and $PM_{2.5}$ over the NCP based on observational data, the validation using numerical model is not included in the current manuscript. This aspect should be addressed in future research.

https://doi.org/10.5194/egusphere-2025-285
Preprint. Discussion started: 18 March 2025

Data availability

NCEP reanalysis 2 data were provided by the NOAA/OAR/ESRL PSL, Boulder, CO, USA, from their Web site at https://psl.noaa.gov/data/gridded/data.ncep.reanalysis2.html (Kanamitsu et al., 2002, last access: 6 September 2021). Monthly boundary layer height data were provided by the European Centre for Medium-Range Weather Forecasts (ECMWF; https://doi.org/10.24381/cds.adbb2d47, Hersbach et al., 2018; last access: 6 September 2024). The monthly $PM_{2.5}$ concentration data can be downloaded from https://zenodo.org/records/4293239 (Yang, 2020; last access: 9 April 2021). The QBO index is available at https://www.geo.fu-berlin.de/en/met/ag/strat/produkte/qbo/index.html (last access: 7 April 2024). The ENSO index can be downloaded at https://www.cpc.ncep.noaa.gov/data/indices/ (last access: 7 April 2024).

Author contributions

XA, LS and WC designed the experiments and carried them out. XA and TM downloaded and analyzed the reanalysis data and prepared all the figures. XD prepared the paper with contributions from all co-authors. LS, WC, and TM revised the paper.

Competing interests

The contact author has declared that none of the authors has any competing interests.

Acknowledgement

This research has been supported by the National Natural Science Foundation of China (grant nos. 42475043, 42275191 and 41721004).

References

Alexander, M. A.: Midlatitude Atmosphere–Ocean Interaction during El Niño. Part I: The North Pacific Ocean, J. Climate, 5, 944–958, doi:10.1175/1520-0442(1992)005<0944:MAIDEN>2.0.CO;2, 1992.

An, X. D., Sheng, L. F., Liu, Q., Li, C., Gao, Y., and Li, J. P: The combined effect of two westerly jet waveguides on heavy haze in the North China Plain in November and December 2015, Atmos. Chem. Phys., 20, 4667–4680, doi:10.5194/acp-20-4667-2020, 2020.

An, X. D., Chen, W., Fu, S., Hu, P., Li, C., and Sheng, L. F.: Possible dynamic mechanisms of high- and low-latitude wave trains over Eurasia and their impacts on air pollution over the North China Plain in early winter, J. Geophys. Res. Atmos., 127, e2022JD036732, doi:10.1029/2022JD036732, 2022a.

https://doi.org/10.5194/egusphere-2025-285
Preprint. Discussion started: 18 March 2025

An, X. D., Wang, F., Sheng, L. F., and Li, C.: Pattern of Wintertime Southern Rainfall and Northern Pollution over Eastern China: The Role of the Strong Eastern Pacific El Niño, J. Climate, 35, 7259–7273, doi:10.1175/JCLI-D-21-0662.1, 2022b.

An, X. D., Sheng, L. F., Li, C., Chen, W., Tang, Y. L., and Huangfu, J. L.: Effect of rainfall-induced diabatic heating over southern China on the formation of wintertime haze on the North China Plain, Atmos. Chem. Phys., 22, 725–738, doi:10.5194/acp-22-725-2022, 2022c.

An, X. D., Chen, W., Sheng, L. F., Li, C., and Ma, T. J.: Synergistic Effect of El Niño and Arctic Sea-Ice Increment on Wintertime Northeast Asian Anomalous Anticyclone and Its Corresponding $PM_{2.5}$ Pollution, J. Geophys. Res. Atmos., 128, e2022JD037840, doi:10.1029/2022JD037840, 2023a.

An, X. D., Sheng, L. F., and Chen, W.: Impact of the strong wintertime East Asian trough on the concurrent PM2.5 and surface O_3 in eastern China, Atmos. Environ., 306, 119846, doi:10.1016/j.atmosenv.2023.119846, 2023b.

Bjerknes, J.: Atmospheric teleconnections from the equatorial Pacific, Mon. Wea. Rev., 97, 163–172, doi:10.1175/1520-0493(1969)097<0163:ATFTEP>2.3.CO;2, 1969.

Cai, Q., Chen, W., Chen, S., Ma, T., and Garfinkel, C. I.: Influence of the Quasi-Biennial Oscillation on the spatial structure of the wintertime Arctic Oscillation. J. Geophys. Res. Atmos., 127(8), e2021JD035564, doi:10.1029/2021jd035564, 2022.

Chang, L. Y., Xu, J. M., Tie, X. X., and Wu, J. B.: Impact of the 2015 El Nino event on winter air quality in China, Sci. Rep., 6, 34275, doi:10.1038/srep34275, 2016.

Chen, W., Takahashi, M., and Graf, H. F.: Interannual variations of stationary planetary wave activity in the northern winter troposphere and stratosphere and their relations to NAM and SST, J. Geophys. Res., 108, 4797, doi:10.1029/2003JD003834, D24, 2003.

Chen, W., Yang, S., and Huang, R.-H.: Relationship between stationary planetary wave activity and the East Asian winter monsoon, J. Geophys. Res., 110, D14110, doi:10.1029/2004JD005669, 2005.

Chen, W., and Li, T.: Modulation of northern hemisphere wintertime stationary planetary wave activity: East Asian climate relationships by the Quasi-Biennial Oscillation. J. Geophys. Res., 112(D20), D20120, doi:10.1029/2007jd008611, 2007.

Cheng, X., Boiyo, R., Zhao, T., Xu, X., Gong, S., Xie, X., and Shang, K.: Climate modulation of Niño3.4 SST-anomalies on air quality change in southern China: Application to seasonal forecast of haze pollution, Atmos. Res., 225, 157–164, doi:10.1016/j.atmosres.2019.04.002, 2019.

Dang, R. and Liao, H.: Severe winter haze days in the Beijing–Tianjin–Hebei region from 1985 to 2017 and the roles of anthropogenic emissions and meteorology, Atmos. Chem. Phys., 19, 10801–10816, doi:10.5194/acp-19-10801-2019, 2019.

Edmon, H. J., Hoskins, B. J., and Mclntyre, M. E.: Eliassen-Palm crosssections for the troposphere, J. Atmos. Sci., 37, 2600–2616, doi:10.1175/1520-0469(1980)037<2600:EPCSFT>2.0.CO;2, 1980.

https://doi.org/10.5194/egusphere-2025-285
Preprint. Discussion started: 18 March 2025

Ern, M., Diallo, M. A., Khordakova, D., Krisch, I., Preusse, P., Reitebuch, O., Ungermann, J., and Riese, M.: The quasi-biennial oscillation (QBO) and global-scale tropical waves in Aeolus wind observations, radiosonde data, and reanalyses, Atmos. Chem. Phys., 23, 9549–9583, https://doi.org/10.5194/acp-23-9549-2023, 2023.

Geng, G., Xiao, Q., Liu, S., Liu, X., Cheng, J., Zheng, Y., Xue, T., Tong, D., Zheng, B., Peng, Y., Huang, X., He, K., and

He, C., Liu, R., Wang, X. M., Liu, S. C., Zhou, T. J., and Liao, W. H.: How does El Niño-southern oscillation modulate the interannual variability of winter haze days over eastern China?, Sci. Total Environ., 651, 1892–1902, doi:10.1016/j.scitotenv.2018.10.100, 2019.

Hersbach, H., Bell, B., Berrisford, P., Biavati, G., Horányi, A., Muñoz Sabater, J., Nicolas, J., Peubey, C., Radu, R., Rozum, I., Schepers, D., Simmons, A., Soci, C., Dee, D., and Thépaut, J.-N.: ERA5 hourly data on single levels from 1979 to present, Copernicus Climate Change Service (C3S) Climate Data Store (CDS) [dataset], doi:10.24381/cds.adbb2d47, 2018 (last access: 6 September 2024).

Holton, J. R., and Tan, H. C.: The influence of the equatorial quasi-biennial oscillation on the global circulation at 50 mb, J. Atmos. Sci., 37(10), 2200–2208, doi:10.1175/1520-0469(1980)037<2200:TIOTEQ>2.0.CO;2, 1980.

Hoskins, B. J., and Ambrizzi, T.: Rossby wave propagation on a realistic longitudinally varying flow, J. Atmos. Sci., 50, 1661–1671, doi:10.1175/1520-0469(1993)050<1661:RWPOAR>2.0.CO;2, 1993.

Jeong, J. I., Park, R. J., and Yeh, S.-W.: Dissimilar effects of two El Niño types on $PM_{2.5}$ concentrations in East Asia, Environ. Pollut., 242, 1395–1403, doi:10.1016/j.envpol.2018.08.031, 2018.

Jing, Q., Sheng, L. F, Zhang, W. H., and An, X. D.: Characteristics of $PM_{2.5}$ and O_3 Pollution and Related Meteorological Impacts in '2+26' Cities of Beijing-Tianjin-Hebei and Its Surrounding Areas from 2018 to 2021, Research of Environmental Sciences, 36, 875–886, doi:10.13198/j.issn.1001-6929.2023.02.03, 2023.

Kang, M. J., Kim, H., and Son, S. W.: QBO modulation of MJO teleconnections in the North Pacific: impact of preceding MJO phases, npj Clim. Atmos. Sci., 7, 12, doi:10.1038/s41612-024-00565-w, 2024.

Kanamitsu, M., Ebisuzaki, W., Woollen, J., Yang, S-K., Hnilo, J. J., Fiorino, M., and Potter, G. L.: NCEP-DOE AMIPII Reanalysis (R-2), B. Am. Meteorol. Soc., 1631–1643, https://doi.org/10.1175/BAMS-83-11-1631, 2002.

Kinnersley, J. S.: Seasonal asymmetry of the low- and middlelatitude QBO circulation anomaly, J. Atmos. Sci., 56, 1140–1153, 1999.

Kinnersley, J. S., and Tung, K. K.: Mechanisms for the extratropical QBO in circulation and ozone, J. Atmos. Sci., 56, 1942–1962, 1999.

Koval, A. V., Gavrilov, N. M., Kandieva, K. K. et al.: Numerical simulation of stratospheric QBO impact on the planetary waves up to the thermosphere, Sci. Rep., 12, 21701, doi:10.1038/s41598-022-26311-x, 2022.

Li, H., Yang, Y., Wang, H., Li, B., Wang, P., Li, J., and Liao, H.: Constructing a spatiotemporally coherent long-term $PM_{2.5}$ concentration dataset over China during 1980–2019 using a machine learning approach, Sci. Total Environ., 765, 144263, doi:10.1016/j.scitotenv.2020.144263, 2021.

Li, S. L., Han, Z., and Chen, H. P.: A comparison of the effects of interannual Arctic sea ice loss and ENSO on winter haze days: Observational analyses and AGCM simulations, J. Meteor. Res., 31, doi:10.1007/s13351-017-7017-2, 820–833, 2017.

Ma, T., Chen, W., Huangfu, J., Song, L., and Cai, Q.: The observed influence of the Quasi-Biennial Oscillation in the lower equatorial stratosphere on the East Asian winter monsoon during early boreal winter, Int. J. Climatol., 41(14), 6254–6269, doi:10.1002/joc.7192, 2021.

Ma, T. J., Chen, W., An, X. D., Garfinkel, C. I., and Cai, Q. Y.: Nonlinear effects of the stratospheric Quasi-Biennial Oscillation and ENSO on the North Atlantic winter atmospheric circulation, J. Geophys. Res. Atmos., 128, e2023JD039537, doi:10.1029/2023JD039537, 2023.

Ma, X., Wang, L., Smith, D., Hermanson, L., Eade, R., Dunstone, N., Hardiman, S., and Zhang, J. K.: ENSO and QBO modulation of the relationship between Arctic sea ice loss and Eurasian winter climate, Environ. Res. Lett., 17, 124016, doi:10.1088/1748-9326/aca4e9, 2022

Nature Geoscience: Editorial: Cleaner air for China, Nat. Geosci., 12, 497, https://doi.org/10.1038/s41561-019-0406-7, 2019.

Philander, S. G. Yamagata, H., T., and Pacanowski, R. C.: Unstable air-sea interactions in the tropics, J. Atmos. Sci., 41, 604–613, doi:10.1175/1520-0469(1984)041<0604:UASIIT>2.0.CO;2, 1984.

Rao, J., Garfinkel, C. I., and White, I. P.: How does the Quasi-Biennial Oscillation affect the boreal winter tropospheric circulation in CMIP5/6 models?, J. Climate, 33(20), 8975–8996, doi:10.1175/JCLI-D-20-0024.1, 2020.

Rasmusson, E. M., and Carpenter, T. H.: Variations in tropical sea surface temperature and surface wind fields associated with the Southern Oscillation/El Niño, Mon. Wea. Rev., 110, 354–384, doi:https://doi.org/10.1175/1520-0493(1982)110<0354:VITSST>2.0.CO;2, 1982.

Shi, L., Steenland, K., Li, H., Liu, P., Zhang, Y., Lyles, R. H., Requia, W. J., Ilango, S. D., Chang, H. H., Wingo, T., Weber, R. J., and Schwartz, J.: A national cohort study (2000–2018) of long-term air pollution exposure and incident dementia in older adults in the United States, Nat. Commun., 12, 6754, doi:10.1038/s41467-021-27049-2, 2021.

Takaya, K. and Nakamura, H.: A formulation of a phase independent wave-activity flux for stationary and migratory quasigeostrophic eddies on a zonally varying basic flow, J. Atmos. Sci., 58, 608–627, doi:10.1175/15200469(2001)058<0608:AFOAPI>2.0.CO;2, 2001.

Wang, B., Wu, R., and Fu, X.: Pacific-East Asian teleconnection: How does ENSO affect East Asian climate?, J. Climate, 13, 1517–1536, doi:10.1175/1520-0442(2000)013<1517:PEATHD>2.0.CO;2, 2000.

https://doi.org/10.5194/egusphere-2025-285
Preprint. Discussion started: 18 March 2025

Wang, H., Rao, J., Guo, D., Liu, Y., and Liu, Y.: Linear interference between effects of ENSO and QBO on the northern winter stratospheric polar vortex, Clim. Dyn., doi:10.1007/s00382-023-07040-x, 2023.

Wang, J, Liu, Y. J., Ding, Y. H., Wu, P., Zhu, Z. W., Xu, Y., Li, Q. P., Zhang, Y. X., He, J. H., Wang, J. L. X. L., and Qi, L.: Impacts of climate anomalies on the interannual and interdecadal variability of autumn and winter haze in North China: A review, Int. J. Climatol., 40, 4309– 4325, 10.1002/joc.6471, 2020.

Wei, K., Chen, W., and Huang, R.: Association of tropical Pacific sea surface temperatures with the stratospheric Holton-Tan Oscillation in the Northern Hemisphere winter, Geophys. Res. Lett., 34(16), L16814, doi:10.1029/2007gl030478, 2007.

Wu, Y., Liu, R., Li, Y., Dong, J., Huang, Z., Zheng, J., and Liu, S. C.: Contributions of meteorology and anthropogenic emissions to the trends in winter $PM_{2.5}$ in eastern China 2013–2018, Atmos. Chem. Phys., 22, 11945–11955, doi:10.5194/acp-22-11945-2022, 2022.

Xie, B. Y., Yang, Y., Wang, P. Y., and Liao, H., Impacts of ENSO on wintertime $PM_{2.5}$ pollution over China during 2014–2021, Atmos. Ocean Sci. Lett., 15, 100189, doi:10.1016/j.aosl.2022.100189, 2021.

Yang, Y.: Constructing a spatiotemporally coherent longterm $PM_{2.5}$ concentration dataset over China during 1980–2019 using a machine learning approach (version 1) [dataset], doi:10.5281/zenodo.4293239, 2020 (last access: 9 April 2021).

Yu, S., and Sun, J. Q.: Potential factors modulating ENSO's influences on the East Asian trough in boreal winter, Int. J. Climatol., 40, 5066–5083, doi:10.1002/joc.6505, 2020.

Yuan, X.: ENSO-related impacts on Antarctic sea ice: A synthesis of phenomenon and mechanisms, Antarct. Sci., 16, 415–425, doi:10.1017/S0954102004002238, 2004.

Yin, Z. C., Zhou, B. T., Chen, H. P., and Li, Y. Y.: Synergetic impacts of precursory climate drivers on interannual-decadal variations in haze pollution in North China: A review, Sci. Total Environ., 755, 143017, doi:10.1016/j.scitotenv.2020.143017, 2021.

Zeng, L., Yang, Y., Wang, H., Wang, J., Li, J., Ren, L., Li, H., Zhou, Y., Wang, P., and Liao, H.: Intensified modulation of winter aerosol pollution in China by El Niño with short duration, Atmos. Chem. Phys., 21, 10745–10761, https://doi.org/10.5194/acp-21-10745-2021, 2021.

Zhang, G., Gao, Y., Cai, W., Leung, L. R., Wang, S., Zhao, B., Wang, M., Shan, H., Yao, X., and Gao, H.: Seesaw haze pollution in North China modulated by the sub-seasonal variability of atmospheric circulation, Atmos. Chem. Phys., 19, 565–576, doi:10.5194/acp-19-565-2019, 2019.

Zhang, R. H., Akimasa, S., and Masahide, K.: Impact of El Niño on the East Asian Monsoon: A diagnostic study of the '86/87' and '91/92'events, J. Meteor. Soc. Japan, 74, 49–62, doi:10.2151/jmsj1965.74.1_49, 1996.

https://doi.org/10.5194/egusphere-2025-285
Preprint. Discussion started: 18 March 2025

Zhang, R. H., and Akimasa, S.: Moisture circulation over East Asia during El Niño episode in Northern winter, spring and autumn, J. Meteor. Soc. Japan, 80, 213–227, doi:10.2151/jmsj.80.213, 2002.

Zhang, R. H., Zhou, W., Tian, W. S., Zhang, Y., Jian, Y. T., Li., Y. N.: Tropical Stratospheric Forcings Weaken the Response of the East Asian Winter Temperature to ENSO, Ocean-Land-Atmos Res., 2, 0001, doi:10.34133/olar.0001, 2023.

Zhang, R., and Zhou, W.: Decadal Change in the Linkage between QBO and the Leading Mode of Southeast China Winter Precipitation, J. Climate, 36(21), 7379–7392, doi:10.1175/JCLI-D-23-0028.1, 2023.

Zhang, S. Y., Zeng, G., Yang, X. Y., and Iyakaremye, V.: Two leading patterns of winter $PM_{2.5}$ variations in eastern China before the outbreak of cold surge and their causes, Atmos. Res., 287, 106696, doi:10.1016/j.atmosres.2023.106696, 2023.

Zhang, S. Y., Zeng, G., Yang, X. Y., and Wang, T. J.: Opposite trends of cold surges over South China Sea and Philippines Sea and their different impacts on $PM_{2.5}$ in eastern China, Sci. Total Environ., 908, 168454, doi:10.1016/j.scitotenv.2023.168454, 2024.

Zhang, Q.: Tracking Air Pollution in China: Near Real-Time PM2.5 Retrievals from Multisource Data Fusion. Environ, Sci. Technol., 55, 12106–12115, doi:10.1021/acs.est.1c01863, 2021.

Zhao, S., Feng, T., Tie, X., Long, X., Li, G., Cao, J., Zhou, W., and An, Z.: Impact of Climate Change on Siberian High and Wintertime Air Pollution in China in Past Two Decades, Earth's Future, 6, 118–133, doi:10.1002/2017EF000682, 2018.

Zhao, S., Feng, T., Tie, X., Li, G., and Cao, J.: Air pollution zone migrates south driven by East Asian winter monsoon and climate change, Geophys. Res. Lett., 48, e2021GL092672, doi:10.1029/2021GL092672, 2021.

Zhao, W., Chen, S., Zhang, H., Wang, J., Chen, W., Wu, R., Xing, W., Wang, Z., Hu, P., Piao, J., and Ma, T.: Distinct Impacts of ENSO on Haze Pollution in the Beijing–Tianjin–Hebei Region between Early and Late Winters, J. Climate, 35, 687–704, doi:10.1175/JCLI-D-21-0459.1, 2022.

Zhong, J., Zhang, X., Gui, K., Liao, J., Fei, Y., Jiang, L., Guo, L., Liu, L., Che, H., Wang, Y., Wang, D., and Zhou, Z.: Reconstructing 6-hourly $PM_{2.5}$ datasets from 1960 to 2020 in China [dataset], doi:10.5281/zenodo.6372847, 2022a (last access: 30 March 2022).

Zhong, J., Zhang, X., Gui, K., Liao, J., Fei, Y., Jiang, L., Guo, L., Liu, L., Che, H., Wang, Y., Wang, D., and Zhou, Z.: Reconstructing 6-hourly $PM_{2.5}$ datasets from 1960 to 2020 in China, Earth Syst. Sci. Data, 14, 3197–3211, doi:10.5194/essd-14-3197-2022, 2022b.

Zhou, Y., Zhang, H., Parikh, H. M., Chen, E. H., Rattanavaraha, W., Rosen, E. P., Wang, W. X., and Kamens, R.: Secondary organic aerosol formation from xylenes and mixtures of toluene and xylenes in an atmospheric urban hydrocarbon mixture: Water and particle seed effects (II), Atmos. Environ., 45, 3882–3890, doi:10.1016/j.atmosenv.2010.12.048, 2011.

https://doi.org/10.5194/egusphere-2025-285
Preprint. Discussion started: 18 March 2025

Zhou, Z.-Q., Xie, S.-P., Zheng, X.-T., Liu, Q. Y., and Wang, H.: Global warming–induced changes in El Niño teleconnections over the North Pacific and North America, J. Climate, 27, 9050–9064, doi:10.1175/JCLI-D-14-00254.1, 2014.

https://doi.org/10.5194/egusphere-2025-285
Preprint. Discussion started: 18 March 2025

Table 1: Years of QBO and ENSO events based on the QBO index and ENSO events in November to December during the Period of 1979–2019.

	EQBO	Neutral	WQBO
El Niño	1986, 1997, 2002, 2004, 2006, 2009, 2015	/	1979, 1982, 1987, 1991, 1994, 2014, 2018
Neutral	1980, 1981, 1985, 1990, 1993, 2013, 2019	/	1989, 1992, 1996, 2001, 2003, 2012
La Niña	1983, 1988, 1995, 1999, 2008, 2011, 2017	2000	1984, 1998, 2005, 2007, 2010, 2016

https://doi.org/10.5194/egusphere-2025-285
Preprint. Discussion started: 18 March 2025

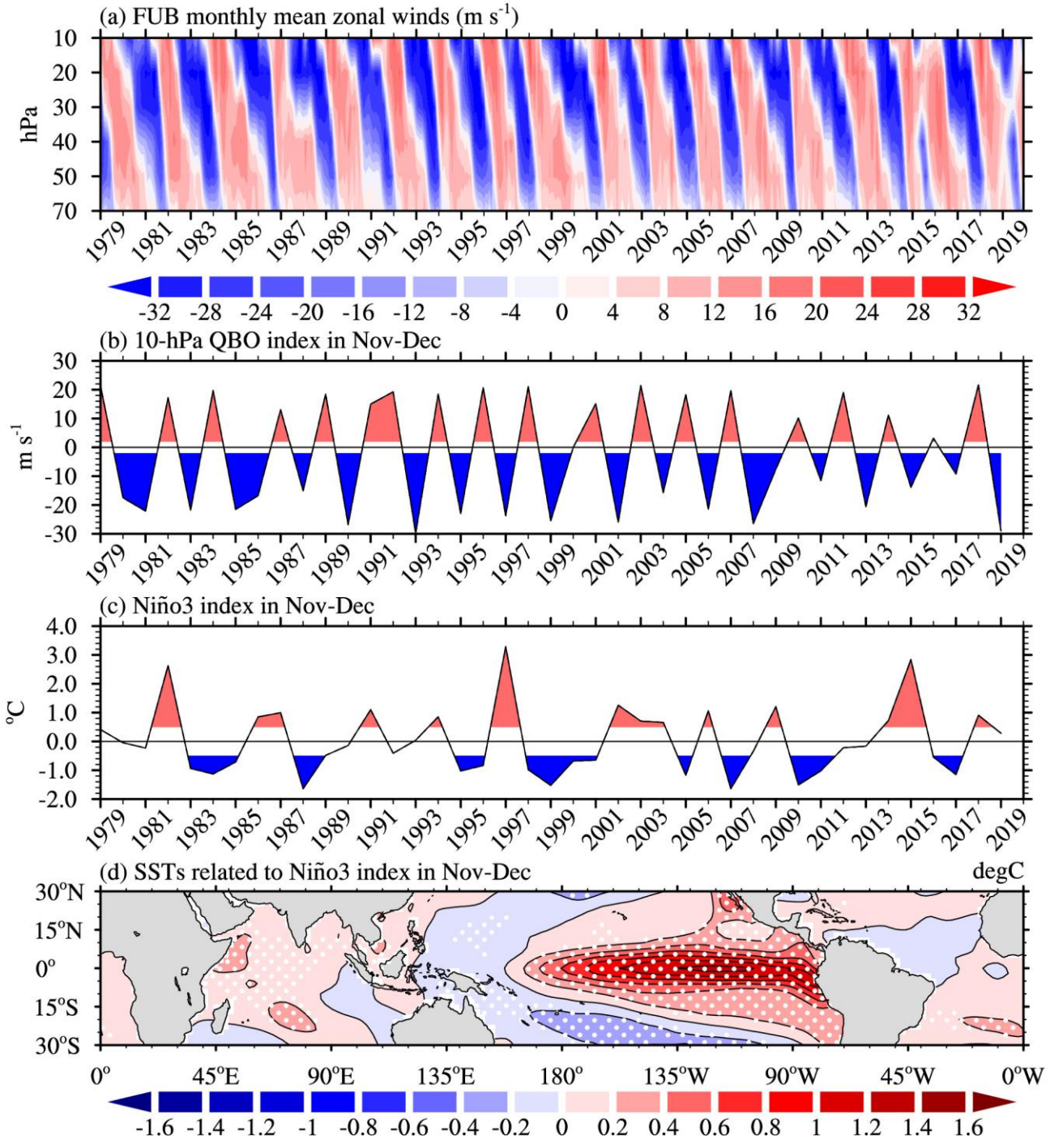

Figure 1: (a) Time-height cross-section of the monthly mean equatorial zonal winds provided by the FUB (unit: m s^{-1}); (b–c) Time series of the 10-hPa QBO and Niño3 indices, averaged in the early winter months (ND); (d) Regression coefficients of SST anomalies onto the Niño3 index shown in (c). White dots indicate where values are significant at the 99% confidence level.

https://doi.org/10.5194/egusphere-2025-285
Preprint. Discussion started: 18 March 2025

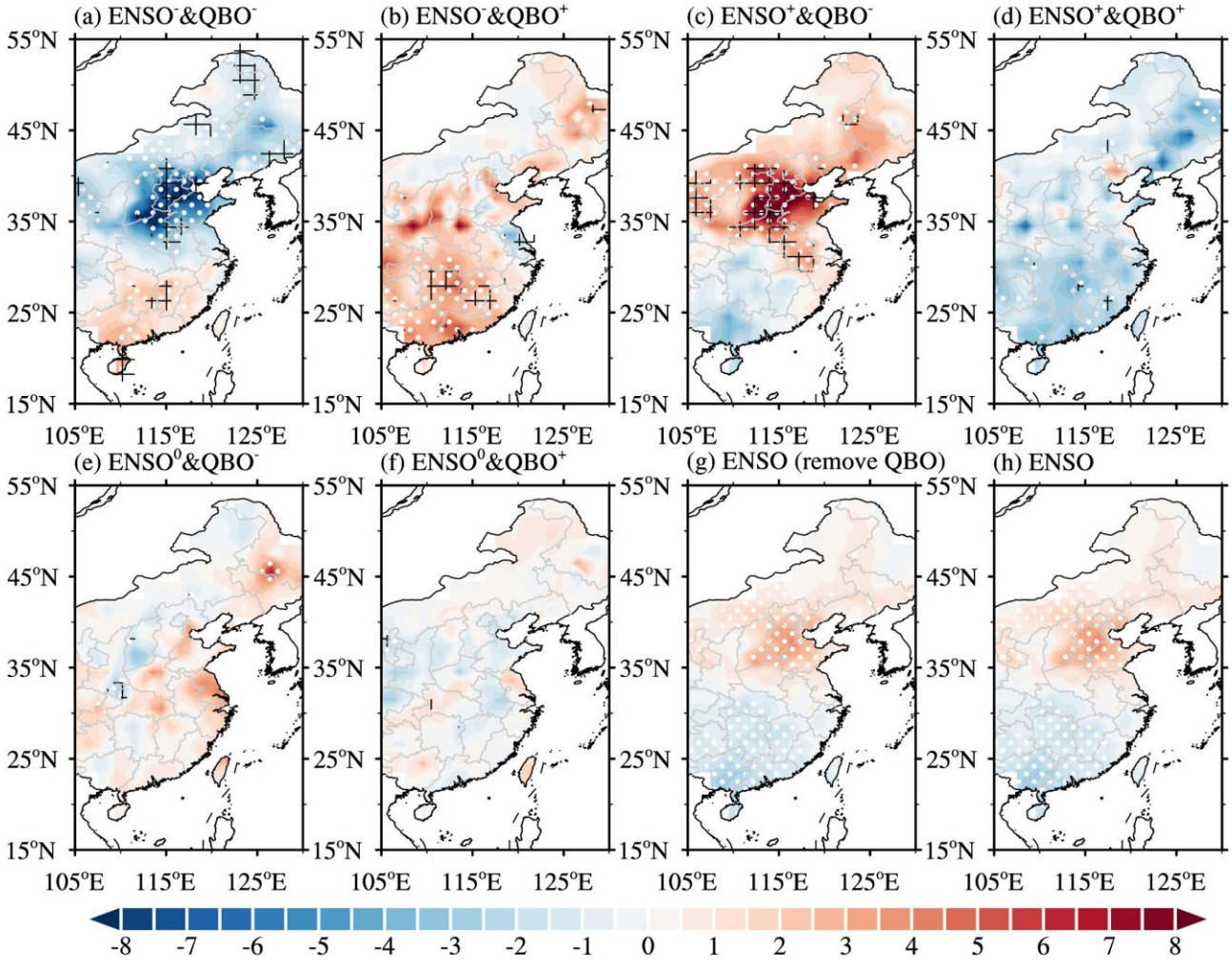

Figure 2: Composite patterns of anomalous $PM_{2.5}$ concentrations (shading; unit: μg m^{-3}) for (a) La Niña & EQBO, (b) La Niña & WQBO, (c) El Niño & EQBO, (d) El Niño & WQBO, (e) nENSO & EQBO, (f) nENSO & WQBO; (g–h) Regression coefficients of anomalous $PM_{2.5}$ concentrations onto the Niño3 index (QBO signals removed), and Niño3 index shown in Figs. 1b and c. White dots indicate areas of significant at the 90% confidence level.

https://doi.org/10.5194/egusphere-2025-285
Preprint. Discussion started: 18 March 2025

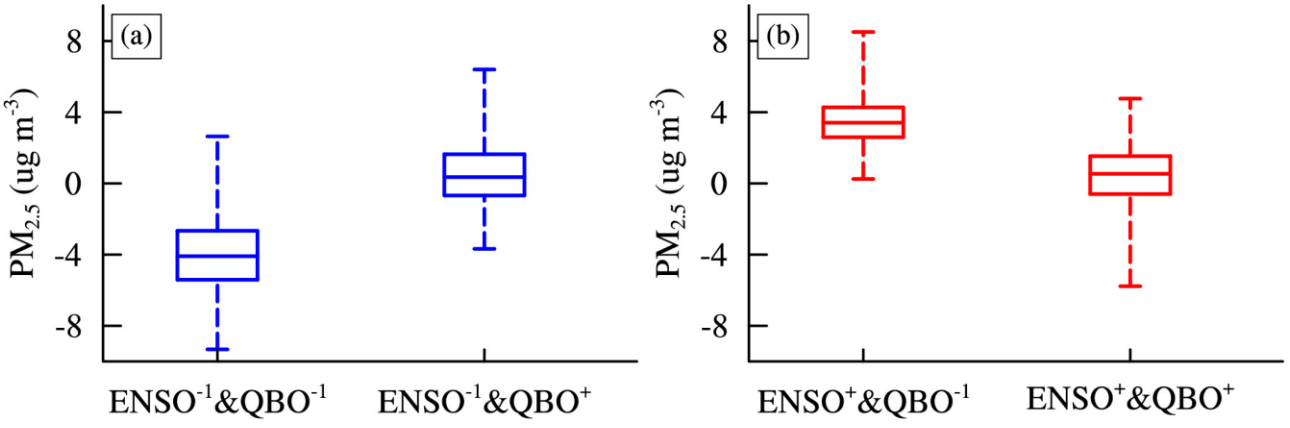

Figure 3: The average-mean $PM_{2.5}$ concentration anomalies over the NCP (32°N–42°N, 110°E–120°E) for (a) La Niña & EQBO and La Niña & WQBO; (b) El Niño & EQBO and El Niño & WQBO. Boxplots are drawn based on 1,000 resamples using the bootstrap method.

https://doi.org/10.5194/egusphere-2025-285
Preprint. Discussion started: 18 March 2025

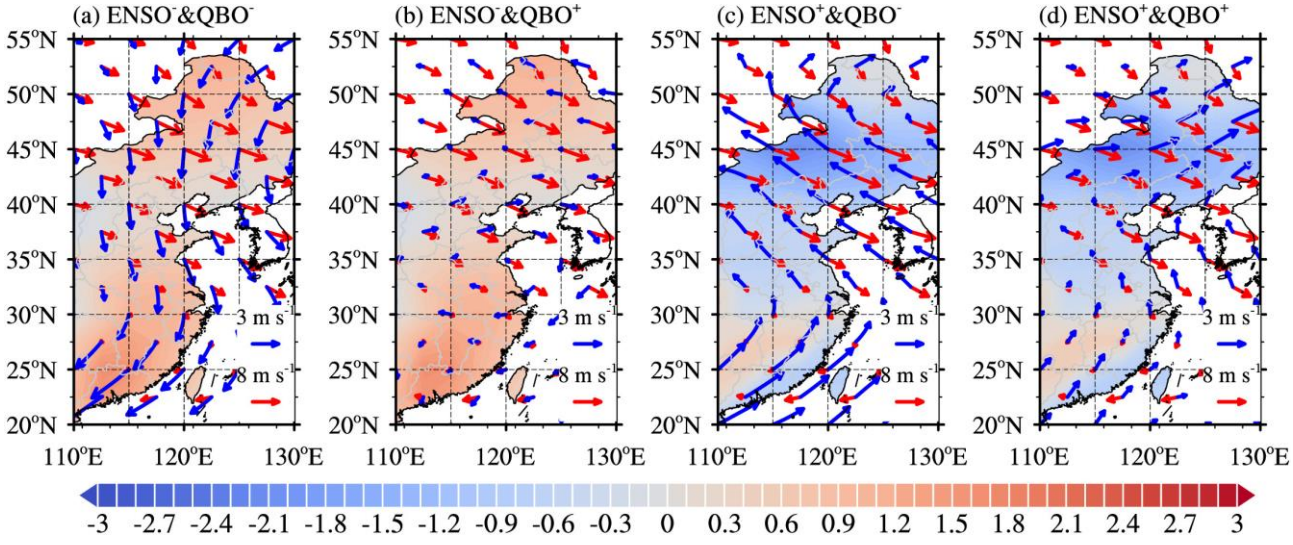

Figure 4: Composite patterns of wind fields at 850 hPa. Red vectors represent climatological winds, and blue arrows represent anomalous winds for (a) La Niña and EQBO, (b) La Niña and WQBO, (c) El Niño and EQBO, and (d) El Niño and WQBO. Shaded areas in (a–b) and (c–d) represent the differences in 850-hPa wind speed between La Niña & EQBO and La Niña & WQBO, and between El Niño & EQBO and El Niño & WQBO, respectively.

https://doi.org/10.5194/egusphere-2025-285
Preprint. Discussion started: 18 March 2025

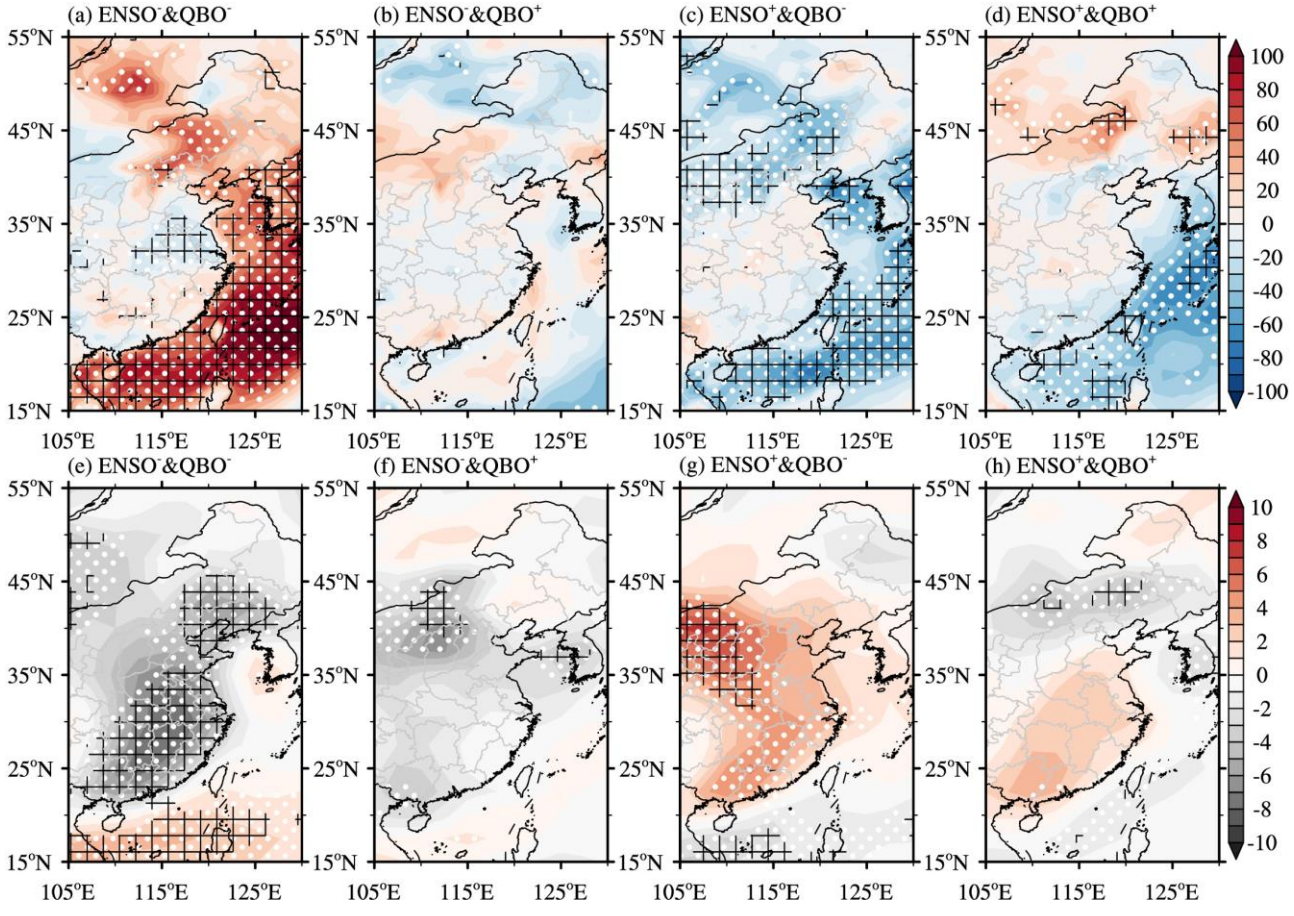

Figure 5: Same as Figure 4, but for (a–d) boundary layer height anomalies and (e–f) 925-hPa relative humidity anomalies. White dotted (black grid) areas indicate significant values at the 80% (90%) confidence level.

https://doi.org/10.5194/egusphere-2025-285
Preprint. Discussion started: 18 March 2025

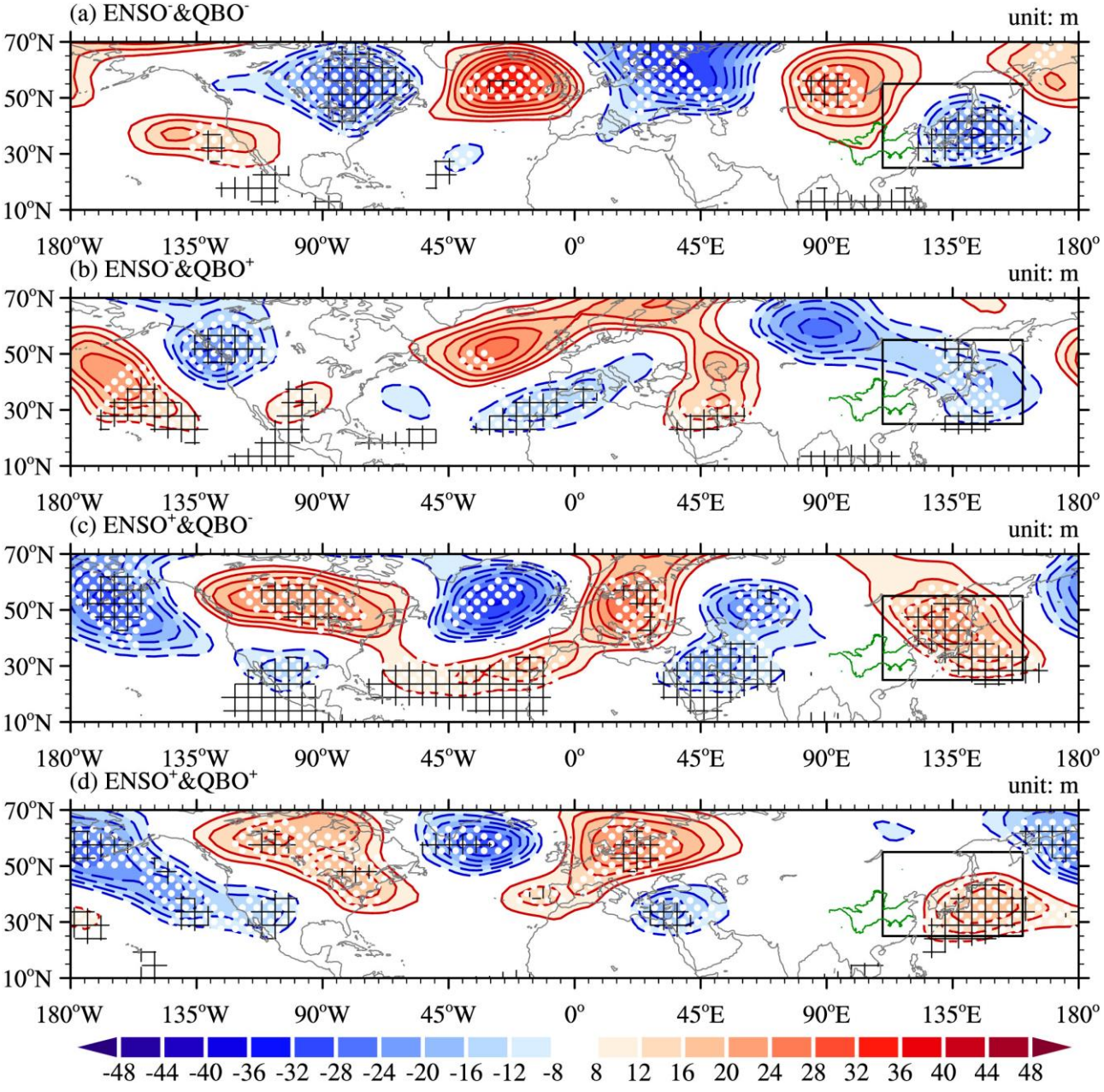

Figure 6: Same as Figure 4, but for geopotential height anomaly at 500 hPa. White dotted (black grid) areas indicate significant values at the 80% (90%) confidence level. The black box represents the key region of the northeast Asian anomalous anticyclone, as defined by An et al. (2023a).

https://doi.org/10.5194/egusphere-2025-285
Preprint. Discussion started: 18 March 2025

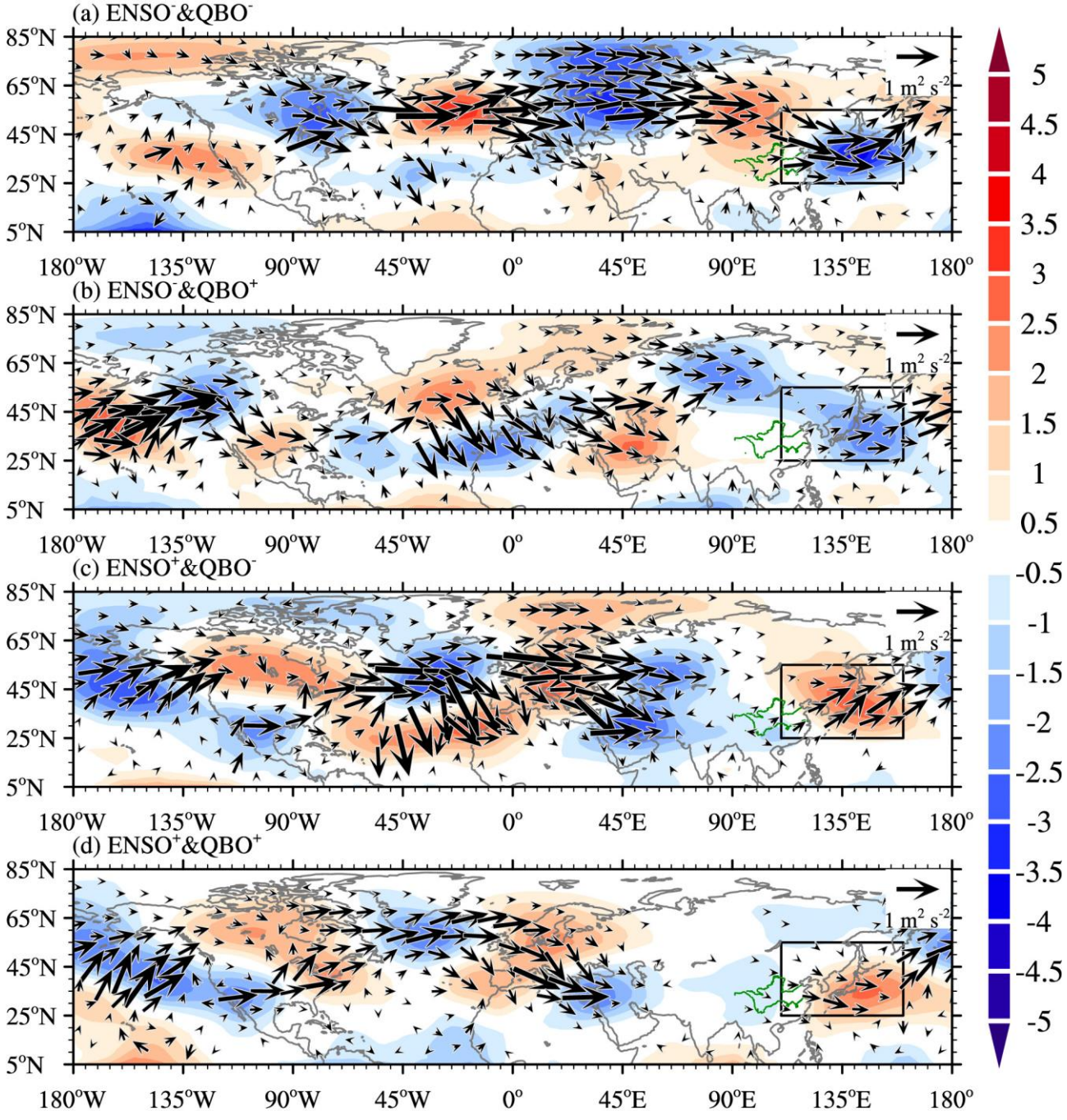

460 **Figure 7: Same as Figure 6, but for disturbed streamfunction (contours; unit:10^6 m^2 s^{-1}; interval: 1) and wave activity flux (vectors; unit: m^2 s^{-2}) at 500 hPa.**

https://doi.org/10.5194/egusphere-2025-285
Preprint. Discussion started: 18 March 2025

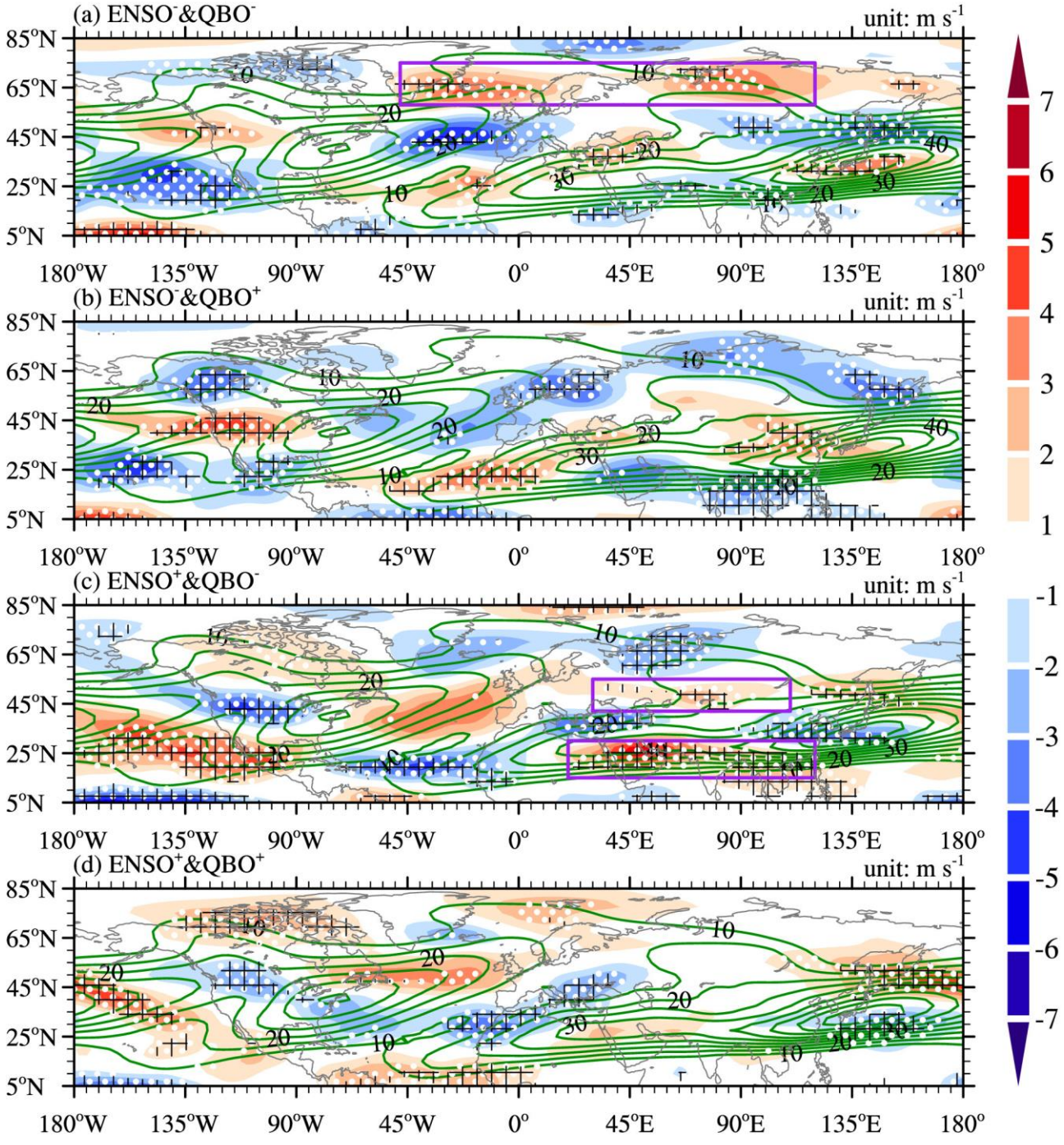

Figure 8: Same as Figure 6, but for climatological zonal winds (green contours; unit: m s^{-1}; interval: 5) and zonal wind anomalies (shading; unit: m s^{-1}) at 300 hPa. White dotted (black grid) areas indicate significant values at the 80% (90%) confidence level. Purple boxes represent the key regions of zonal wind changes.

https://doi.org/10.5194/egusphere-2025-285
Preprint. Discussion started: 18 March 2025

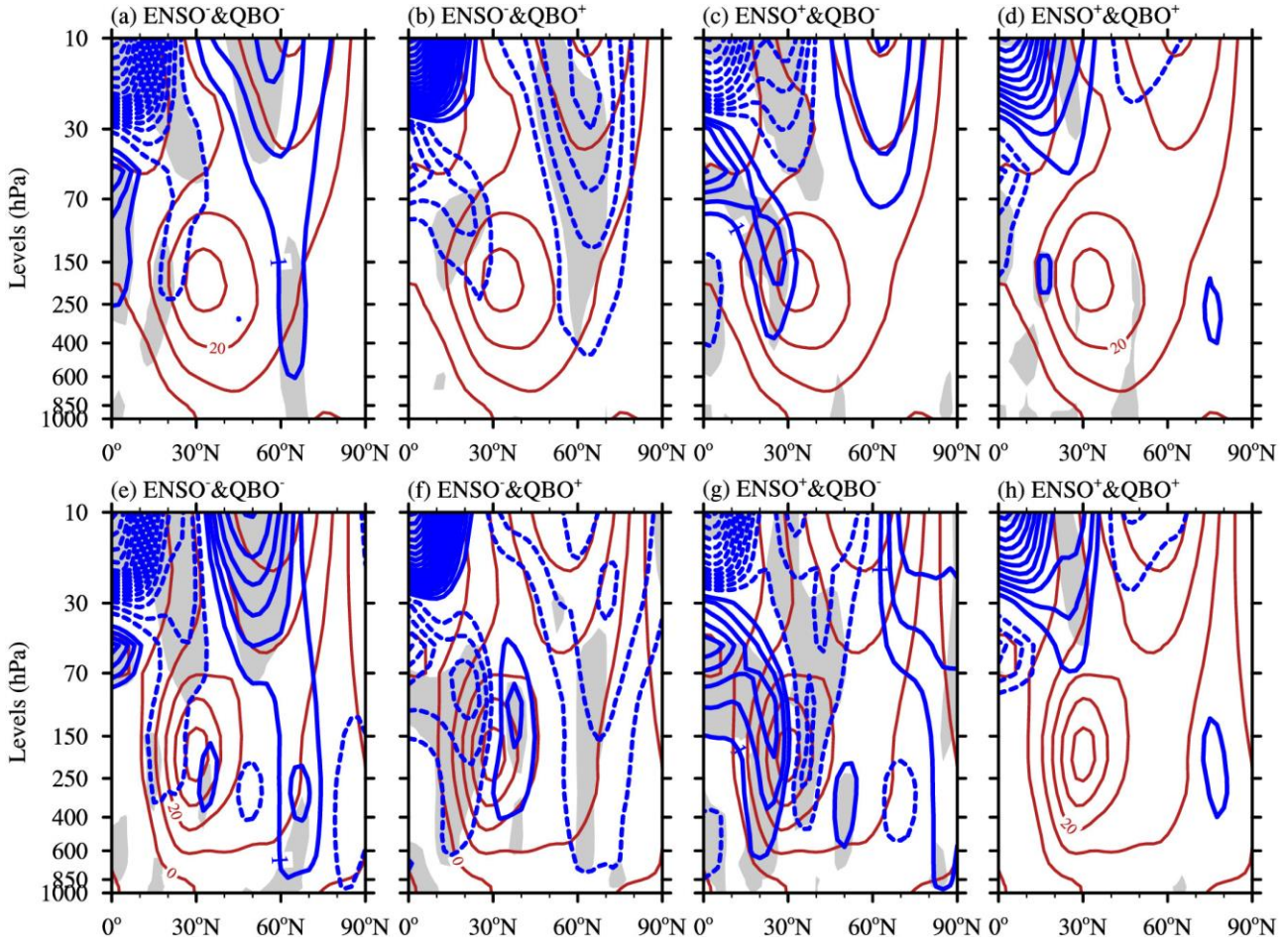

Figure 9: Climatological mean of the zonal-mean zonal winds (red contours; unit: m s^{-1}) and composite zonal-mean zonal winds (blue contours; unit: m s^{-1}) in 0°–360°E for (a) La Niña and EQBO, (b) La Niña and WQBO, (c) El Niño and EQBO, and (d) El Niño and WQBO. (e)–(f) Same as (a)–(d), but for zonal winds averaged in 0°–140°E. Grey shaded areas indicate significant values at the 90% confidence level.

https://doi.org/10.5194/egusphere-2025-285
Preprint. Discussion started: 18 March 2025

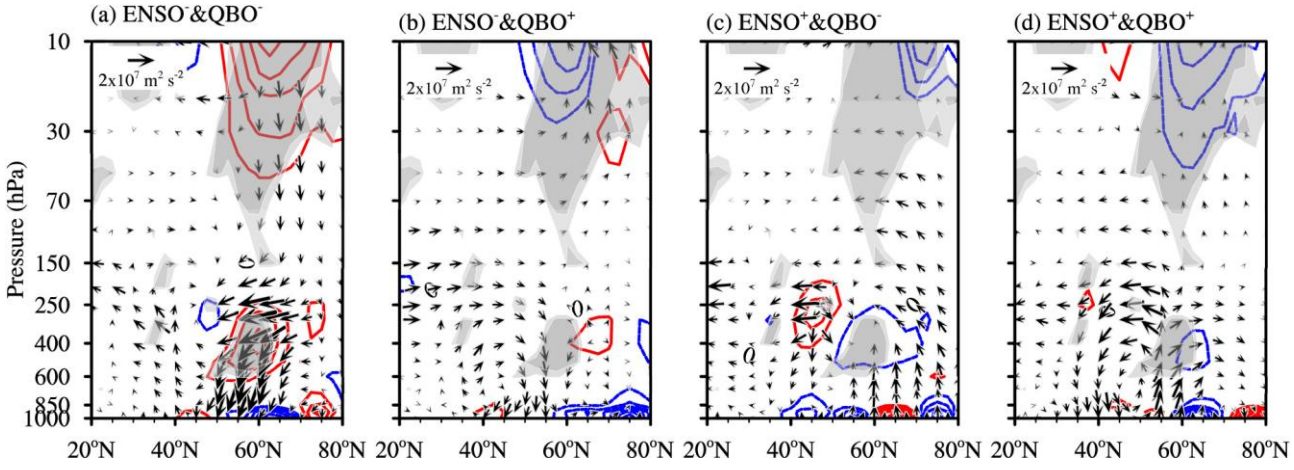

Figure 10: Cross-sections of the EP flux (vectors; unit: $m^2\ s^{-2}$) for waves 1–2 and its divergence (contours, with red (blue) lines represent divergence (convergence); unit: $m\ s^{-1}\ day^{-1}$) for (a) La Niña and EQBO, (b) La Niña and WQBO, (c) El Niño and EQBO, and (d) El Niño and WQBO. Heavy and light shaded areas indicate significant values at the 95% and 90% confidence levels, respectively.